

# White dwarf stars as strange quark matter detectors – II

O. G. Benvenuto<sup>1,2★†</sup>

<sup>1</sup>*Departamento de Astronomía y Astrofísica, Pontificia Universidad Católica, Vicuña Mackenna 4860, Casilla 306, Santiago, Chile*

<sup>2</sup>*Facultad de Ciencias Astronómicas y Geofísicas, Universidad Nacional de La Plata, Paseo del Bosque S/N, B1900FWA, La Plata, Argentina*

Accepted 2005 December 30. Received 2005 December 27; in original form 2005 October 27

## ABSTRACT

We study the properties of the non-radial pulsations of strange dwarf stars. These objects are white dwarfs (WDs) with a compact core made up of strange quark matter (SQM). We show that the SQM core compresses the surrounding normal matter strongly enough to give rise to the occurrence of a sharp peak in the Brunt–Väisälä frequency. This, in turn, allows for the existence of a completely new resonant cavity for gravity (g-) modes, which is absent in standard WDs. We study the cases in which the mass of the SQM core is  $10^{-2}$ ,  $10^{-3}$ ,  $10^{-4}$  and  $10^{-5}$  of the total stellar mass, which have been added to a  $0.525 M_{\odot}$  WD model adequate to account for the period structure of the DAV G117B15A, showing that this new resonant cavity is present for such a large range of core mass fractions.

Due to the extremely short wavelength of g-modes in the new resonant cavity, we treat oscillations there with an asymptotic analysis up to an intermediate, evanescent zone (located at  $\approx 10$  per cent of the stellar radius). At such a point, we consider the asymptotic treatment as a boundary condition for a self-consistent numerical calculation of the g-mode spectrum of oscillations. In particular, we consider dipolar oscillations, which are currently identified with the observed oscillations in standard WDs. We find a very distinctive signal for the presence of a SQM core inside a WD: the difference of periods between two consecutive modes is far shorter than it is in standard WDs due to the oscillations in the new resonant cavity, being even shorter than a second. This confirms previous expectations based on very simplified calculations.

Our calculations indicate that, while the period spacing between consecutive modes is a smooth function of the period, the square of the amplitude of the modes near the SQM core is a strongly varying function. While some modes will have large amplitude there, and thus large kinetic energy, others will have far lower energy. Then, if (as usual) we assume that the excited modes are those with low kinetic energy, we expect a very particular spectrum of dipolar oscillations of WDs with SQM cores. The spectrum should be characterized by several well-detached sets of a very large number of evenly (in period) spaced modes. This should be considered as a clearly distinctive, observable signature of the presence of SQM inside WDs.

**Key words:** dense matter – stars: oscillations – white dwarfs.

## 1 INTRODUCTION

Strange quark matter (SQM) is a particular form of quark matter with a high content of strangeness per baryon  $s/n_B \approx -1$  that has attracted the attention of researchers since the proposal that it may be the actual ground state of hadronic matter (Bodmer 1971; Terazawa 1979; Witten 1984). As a natural consequence of such a proposal, it has been envisaged that the currently called neutron stars should

be in fact made up of SQM. These hypothetical objects have been called strange stars [see Alcock & Olinto (1990) and references therein]. Other situations of astrophysical interest at which SQM could play a role are during the explosion of a massive star as a supernova. It has been proposed that the combustion from nuclear matter to SQM is not possible by means of deflagration (Horvath & Benvenuto 1988) but by detonation (Benvenuto & Horvath 1989). This detonation wave may be the ultimate reason of the occurrence of these theoretically elusive explosions. While this exotic mechanism was proposed long ago in order to circumvent problems with the explosion mechanism of such stars, state-of-the-art models based on standard physics still fail to explode (Buras et al. 2003).

★E-mail: obenvenu@astro.puc.cl, obenvenu@fcaglp.unlp.edu.ar

†Member of the Carrera del Investigador Científico, Comisión de Investigaciones Científicas de la Provincia de Buenos Aires (CIC), Argentina

Remarkably, if SQM were the actual ground state for strongly interacting matter, we should expect it to be found even at zero pressure, and then it is a natural candidate for dark matter (Witten 1984). An obvious major problem in this line of research is to find ways to prove the actual existence of SQM somewhere in the Universe.

Recently, some observations (see e.g. Li et al. 1999; Drake et al. 2002) indicate that the radius of some compact stars is so small that they are in conflict with standard neutron star models. In these cases, it has been suggested that the unexpected compactness of these objects can be accounted for if they are made up not by neutron matter but by SQM. This has again sparked the interest on the possibility of the actual existence of SQM. Note that, if SQM were absolutely stable, we would expect the existence of bare strange stars (e.g. Page & Usov 2002; Xu 2002) in which the quark matter surface is in direct contact with vacuum.

An interesting proposal for a place at which such an exotic substance may exist is at the interior of the so-called strange dwarfs (hereafter SDs). These objects are white dwarf stars (WDs) with a small core of SQM (Glendenning, Kettner & Weber 1995a,b; Vartanyan, Grigoryan & Sargsyan 2004). As SQM can coexist with normal matter if it has a density below that corresponds to neutron drip ( $\rho_{\text{drip}} \approx 4 \times 10^{11} \text{ g cm}^{-3}$ ), we may expect the existence of objects with a SQM core with a mass value between zero (a standard WD) and a critical value for which normal matter in hydrostatic equilibrium has a density equal to  $\rho_{\text{drip}}$ . If normal matter were at even higher densities, we would have an unstable situation in which the whole star would be converted to SQM in a very energetic event.

Regarding the way a WD may convert into a SD, we consider the most probable way that the star in some previous evolutionary stage accretes chunks of SQM coming from the interstellar medium. If this were the case, SDs would be useful to perform indirect estimations of the density of chunks of SQM and its viability as dark matter candidate. Note that SQM is a possible ground state of dense matter for chunks of total baryon number larger than  $\approx 100$  (see e.g. Farhi & Jaffe 1984). Due of this reason, we consider it not possible a spontaneous decay to SQM of more than  $\approx 100$  baryons in the core of a WD. Such a decay is strongly suppressed because of the absence of strange quarks in nuclei inside standard WDs.

The most direct way in which we could expect to differentiate SDs from standard WDs is by comparing the mass–radius relation for both objects. At present, the radii of some WDs have been measured rather accurately and, in principle, they may be expected to be useful for such a comparison. It has been shown that SDs are more compact than a WD of the same mass *and* internal chemical composition; however the difference in the radius is too small to be useful in getting conclusive evidence in favour of the existence of SDs [see the results presented in Panei, Althaus & Benvenuto (2000) and Vartanyan et al. (2004)].

In principle, we could expect a very different cooling history for these two kinds of dwarfs, but this has been shown not to be the case, since the evolution is very similar to the standard one corresponding to WDs (Benvenuto & Althaus 1996a,b). Thus, WD population studies are of little help for our purposes. However, this is not the case regarding the non-radial pulsations of these stars.<sup>1</sup>

<sup>1</sup> It is worth remarking here that *radial* pulsations of SDs have been studied in the papers proposing the existence of SDs (Glendenning et al. 1995a,b). In these works, the main aim of such a study was to test the stability of these configurations. In any case, radial pulsations are not useful for comparing with observations because the observed range of periods in compact, degenerate variable stars should correspond to gravity (g) modes. Up to now,

Pulsations are very sensitive to the density profile and, as we will show below, provide a very interesting test to perform. It is the aim of this work to study the properties of non-radial pulsations of SDs, in particular its spectrum of oscillations. A short, exploratory study of the problem addressed in this paper can be found in Benvenuto (2005, hereafter Paper I).

The referred spectrum of oscillations has been observed in some variable stars, and it is usually attributed to pulsating WDs, but may also correspond to SDs. Although the treatment to be presented in this paper is only possible in pulsating WDs, we should remark that there is no obvious reason to expect variable WDs to be a special kind of WDs. Thus, variability is expected to be a common phenomenon for all WDs as they cool down across the interval of effective temperatures at which oscillations are observed (the so-called instability strip).

There are two kinds of observed degenerate variable stars usually identified as WDs. DAVs correspond to objects with hydrogen-rich outermost envelopes, whereas the DBVs have helium envelopes. Because the majority of observed WDs belong to DAVs, in this work we will be concerned with stellar models with hydrogen dominated outer envelopes. Worth noting, for example, is the case of G117B15A, which may be considered as the best-studied DAV WD. It has three periods, 215, 271 and 307 s, that are interpreted (Bradley 1998; Benvenuto et al. 2002) to correspond to dipolar oscillations ( $\ell = 1$ , where  $\ell$  is the harmonic degree corresponding to the spherical harmonic  $Y_{\ell,m}(\theta, \phi)$  which describes the angular dependence of the oscillation pattern) with radial orders (number of nodes of the radial part of the eigenfunction)  $k = 2, 3$  and  $4$ , respectively. Notably, it has been possible to detect the secular change of period due to the evolution of the object [ $\dot{P} = (2.3 \pm 1.4) \times 10^{-15} \text{ s s}^{-1}$ ], being one of the very few effects of quiescent stellar evolution detectable on human time-scales (Kepler et al. 2000). Some researchers have been involved in disentangling the structure of G117B15A in terms of a defined internal structure and mass. These studies agree in a model with a carbon–oxygen rich core, surrounded by an almost pure helium layer embracing about 1 per cent of the stellar mass. Finally, the outermost layer is made up almost exclusively of hydrogen and has a mass fraction of about  $10^{-4}$ . The mass of the star has been found to be about  $0.525 M_{\odot}$ , which represents a medium value, and its effective temperature is  $\approx 11\,800 \text{ K}$ .

Since sometime ago, G117B15A has been recognized as a valuable laboratory for non-standard physics. For example, it has been possible to put constraints on the mass of axions (Isern, Hernanz & García-Berro 1992; Córscico et al. 2001), and also bound the possible variation of the value of the gravitational constant (Benvenuto, García-Berro & Isern 2004). The interest in this particular WD is due to not only the high precision of the observations now available, but also the remarkable ability of WDs to show differences in structural and/or evolutionary properties that may reveal the occurrence of exotic physics in their interiors. As a matter of fact, the results we will describe are so different from those expected for standard WDs that they are worth comparison in some way with the whole population of DAVs. In any case, as a starting point, we will consider models of WDs compatible with the observations of G117B15A.

In this work, we will adopt the above-mentioned WD model that fits the pulsational properties of G117B15A, and ‘add’ the exotic core. Then, we evolve the model in the same way as done in Benvenuto & Althaus (1996a,b) down to the corresponding effective

no variability has been detected in such stars that can be attributed to radial pulsations.

temperature, and the computation of pulsational modes is done as described in Córscico et al. (2001). As we will show below, the inclusion of a SQM core in the stellar model will modify the agreement between the theoretical predictions with the observations. We will consider linear, adiabatic, non-radial pulsations and assume that the SQM core does not pulsate, as it is almost incompressible near zero pressure conditions. In some sense, this problem may be associated to the situation in which a massive WD undergoes crystallization as it moves across the instability strip, as it is expected to be the case of BPM 37093 (see e.g. Metcalfe, Montgomery & Kanaan 2004). However, this is not the case: crystallization induces only a tiny density change, and the major differences in the oscillation pattern are due to the elastic properties of the solid. Also, the crystal is expected to grow as the WD cools down, meanwhile the SQM core is expected to remain constant in mass.

We should add a word of caution about this method. In performing this study, we will assume that the chemical composition of the SD is essentially the same as that corresponding to a normal WD star of the same mass. This means that we have assumed that the presence of a SQM core has not had a noticeable effect on the pre-WD evolution of the object. Exploration of this point is beyond the scope of the present work. It is expectable that the chemical composition of the SD will be very dependent on the epoch at which the star accretes the SQM core (if it gets a SQM core this way). In any case, we should remark that the change in the density profile comparing a WD with a SD is so large that a change in the chemical composition will produce a minor effect compared to the ones presented below.

The remainder of this paper is organized as follows. In Section 2, we describe the differential equations of non-radial, linear adiabatic pulsations. In Section 3, we describe the properties of SDs as non-radial, adiabatic pulsators. In Section 4, we describe the asymptotic treatment for the oscillations in the neighbourhood of the compact SQM core. In Section 5, we describe the numerical results for the oscillations of the considered models and, finally, in Section 6 we present the discussion of the results and some concluding remarks. We also present Appendix A with the purpose of showing the actual existence of a resonant cavity for g-modes near the SQM compact core by means of a simplified model.

## 2 THE DIFFERENTIAL EQUATIONS OF NON-RADIAL PULSATIONS

The differential equations that govern linear, non-radial pulsations of spherical stars in the adiabatic approximation are (Unno et al. 1989)

$$x \frac{dy_1}{dx} = (V_g - 3) y_1 + \left[ \frac{\ell(\ell+1)}{C_1 \omega^2} - V_g \right] y_2 + V_g y_3, \quad (1)$$

$$x \frac{dy_2}{dx} = (C_1 \omega^2 - A^*) y_1 + (A^* - U + 1) y_2 - A^* y_3, \quad (2)$$

$$x \frac{dy_3}{dx} = (1 - U) y_3 + y_4, \quad (3)$$

$$x \frac{dy_4}{dx} = U A^* y_1 + U V_g y_2 + [\ell(\ell+1) - U V_g] y_3 - U y_4, \quad (4)$$

where  $x$  is the independent variable defined as  $x = r/R$ ,  $r$  is the radial coordinate and  $R$  is the stellar radius. The dependent variables are defined as

$$y_1 = \frac{\xi_r}{r}, \quad (5)$$

$$y_2 = \frac{1}{g r} \left( \frac{p'}{\rho} + \Phi' \right), \quad (6)$$

$$y_3 = \frac{1}{g r} \Phi', \quad (7)$$

and

$$y_4 = \frac{1}{g} \frac{d\Phi'}{dr}. \quad (8)$$

$\omega$  is given by

$$\omega^2 = \frac{\sigma^2 R^3}{G M_\star}. \quad (9)$$

$\xi_r$  represents the radial displacement of the fluid and  $p'$  and  $\Phi'$  are the Eulerian variations of the equilibrium values of the pressure  $p$  and the gravitational potential  $\Phi$ , respectively.  $g$  is the local acceleration of gravity and  $M_\star$  the stellar mass.  $\omega^2$  is the dimensionless square of the angular frequency of oscillation,  $\sigma^2$ .

The adimensional quantities  $V_g$ ,  $U$ ,  $C_1$  and  $A^*$ , inherent to the non-perturbed model, are defined as

$$V_g = \frac{V}{\Gamma_1} = -\frac{1}{\Gamma_1} \frac{d \ln p}{d \ln r} = \frac{g r}{c^2} = \frac{g r \rho}{\Gamma_1 p}, \quad (10)$$

$$U = \frac{d \ln M_r}{d \ln r} = \frac{4\pi \rho r^3}{M_r}, \quad (11)$$

$$C_1 = \left( \frac{r}{R} \right)^3 \frac{M_\star}{M_r}, \quad (12)$$

$$A^* = \frac{r}{g} N^2 = r \left( \frac{1}{\Gamma_1} \frac{d \ln p}{dr} - \frac{d \ln \rho}{dr} \right). \quad (13)$$

Here,  $\Gamma_1$  is the first adiabatic index,  $c^2$  is the square of the local velocity of sound,  $M_r$  is the mass contained in a (non-perturbed) sphere of radius  $r$  and  $N^2$  is the Brunt–Väisälä frequency.

Equations (1)–(4) have to be supplemented with the adequate boundary conditions. The outer boundary conditions are given by Unno et al. (1989)

$$\begin{aligned} y_1 - y_2 + y_3 &= 0, \\ (\ell + 1) y_3 + y_4 &= 0, \\ y_1 &= 1, \end{aligned} \quad (14)$$

where the last equation is the normalization condition, usually employed in previous works. For the case of the central boundary conditions, these are imposed by the very particular conditions present in SDs. At the last fluid layer of the model (that may be limited by crystallization of the normal matter underlying layer or directly by the SQM core, see below), radial displacement and the perturbation of the gravitational potential must be zero. Thus,

$$y_1 = 0; \quad y_3 = 0. \quad (15)$$

## 3 PROPERTIES OF SD STARS AS NON-RADIAL, ADIABATIC PULSATORS

In order to study the pulsational properties of SDs, we have to employ a detailed stellar model. As described above, we will consider a model of a carbon–oxygen WD of  $0.525 M_\odot$  that has revealed (Benvenuto et al. 2002) as adequate in accounting for the

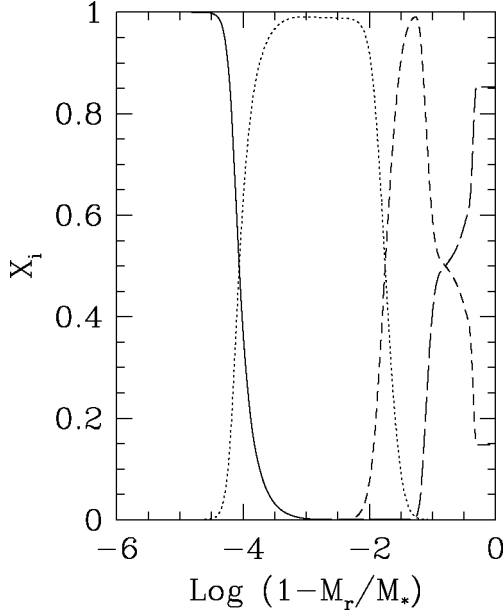


**Figure 1.** The chemical composition (in mass fraction) of the normal matter portion of the models considered here. The star has a thin hydrogen-rich (solid line) layer above a helium layer (dotted line). The stellar core is made up of carbon (short-dashed line) and oxygen (long-dashed line). The SQM core is not included in this figure.

pulsational properties of the well-studied DAV G117B15A.<sup>2</sup> In Fig. 1, we show the chemical profile of the model as a function of its mass. This model is modified by the inclusion of a SQM core. In this paper, we will consider different mass fractions for the SQM core  $Q_{\text{SQM}} \equiv M_{\text{SQM}}/M_*$  where  $M_{\text{SQM}}$  and  $M_*$  are the mass of the SQM core and the mass of the star, respectively. These fractions are  $Q_{\text{SQM}} = 10^{-2}, 10^{-3}, 10^{-4}$  and  $10^{-5}$ . For these values of  $Q_{\text{SQM}}$ , the density  $\rho_B$  at the bottom of the normal matter envelope is  $\log \rho_B = 10.0136, 8.3326, 7.1723$  and  $6.6138$ , respectively (cgs units), while in the case of no SQM core the central density is  $\log \rho_c = 6.3805$ . For models of the mass and chemical composition considered in this paper, we have  $\rho_B \approx \rho_{\text{drip}}$  for  $Q_{\text{SQM}} \approx 5 \times 10^{-2}$ . In this work, we will not consider SQM cores as massive as this because we think it represents an absolute upper limit, unlikely to occur in nature.

As already shown (see e.g. Glendenning et al. 1995a,b; Benvenuto & Althaus 1996a), SDs have a very steep density profile near the SQM compact core. The density profile of the normal matter phase is shown in Fig. 2 for the case of the models considered in this paper. Interestingly, for core mass fraction values in the range considered here, compression of the normal material may be so strong that the lowermost layers may undergo crystallization. Crystallization is due to the Coulomb interactions, whose strength is determined by the coupling constant  $\Gamma$  given (for the case of a one-component plasma) by

$$\Gamma = \frac{(Ze)^2}{akT}, \quad (16)$$

<sup>2</sup> Note, however, that this mass value is somewhat lower than the minimum mass for a carbon–oxygen WD with solar composition (see Han, Podsiadlowski & Eggleton 1994). The issue of the dependence of the value of the minimum mass for a WD of a given chemical composition in the presence of a SQM core is not trivial and would demand a detailed numerical study beyond the scope of the present work.

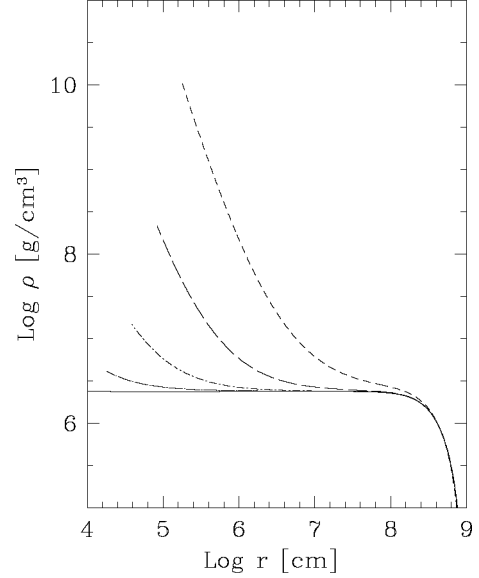


**Figure 2.** The density profile for the normal matter part of models of SDs for the cases in which  $Q_{\text{SQM}} = 10^{-2}, 10^{-3}, 10^{-4}$  and  $10^{-5}$  represented with short dashed, long dashed, dot–short dashed, and dot–long dashed lines, respectively. For comparison, we show the density profile corresponding to a standard WD of the same mass.

where  $Ze$  is the charge of the nucleus and  $a$  the radius of the Wigner–Seitz sphere given by  $4\pi a^3/3 = 1/\rho_n$  ( $\rho_n$  is the nuclei number density).

The critical value for crystallization,  $\Gamma = 171$ , is attained for the case of a  $0.525 M_{\odot}$  SD, even inside the instability strip of hydrogen-rich WDs if  $Q_{\text{SQM}} \gtrsim 5 \times 10^{-4}$ . This interesting behaviour is shown

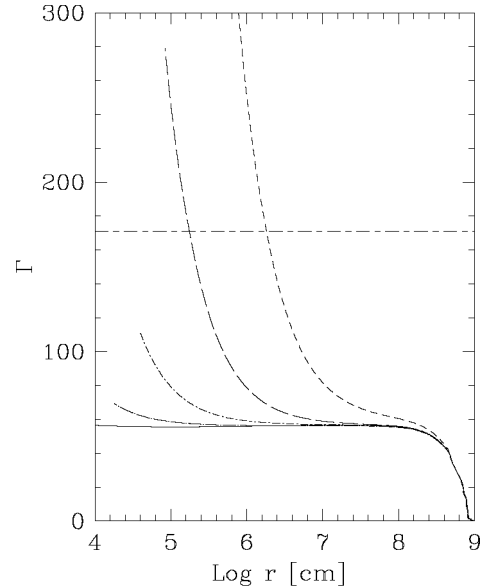


**Figure 3.** The Coulomb coupling constant as a function of the radius of the models for the normal matter part of models of SDs shown in Fig. 2. Lines have the same meaning as there. In solid line, we show the coupling constant for the case of a standard WD of the same mass located inside the instability strip corresponding to DAVs. Horizontal short dash–long dash line represents the critical value of the coupling constant ( $\Gamma = 171$ ) above which normal matter should undergo crystallization.

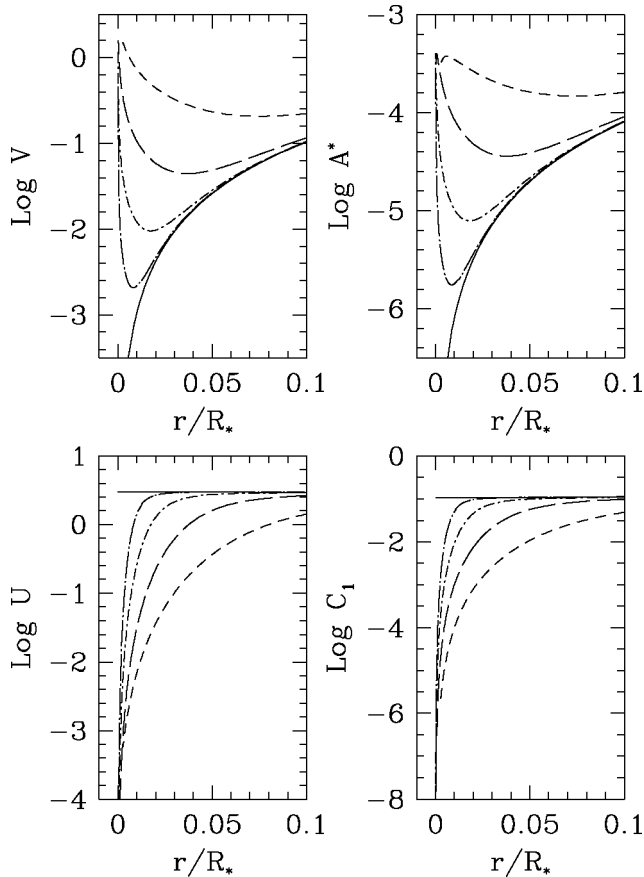


**Figure 4.** The inner profile of the quantities that determine the non-radial pulsation of stellar models as a function of the value of  $Q_{\text{SQM}}$ . Lines have the same meaning as in Fig. 2. We also show the curves corresponding to a standard WD. Note the enormous differences between the profiles of these functions corresponding to SDs and standard WDs. This is the key ingredient in the analysis presented in this paper. For more details, see the main text.

in Fig. 3. For lower  $Q_{\text{SQM}}$  values, the material is fluid for all the normal matter phase of the star. We should remark here that for the case of standard carbon–oxygen, intermediate mass WDs, the onset of crystallization occurs for temperatures far lower than those corresponding to the DAV instability strip.

Now that we have defined the structural properties of the object, we are in a position to study the pulsational properties of the object. The main ingredients are the coefficients of the differential equations (equations 1–4) that determine the non-radial pulsation of the model given above:  $V_g$  (equation 10),  $U$  (equation 11),  $C_1$  (equation 12) and  $A^*$  (equation 13). In Fig. 4, we show the profile of these four quantities as functions of the fractional radius. We note, as it may be expected, that the profiles suffer from enormous variations due to the presence of a SQM dense core as compared with the case of standard WDs. As a matter of fact, the asymptotic behaviour for small values of the radius is completely changed. While in the case of standard WDs (depicted in solid lines in the panels of Fig. 4)  $U$  and  $C_1$  tend to constant values, in the case of SDs, these functions drop precipitously showing a dependence  $\propto r^{-3}$ . The opposite situation is found for  $V_g$  and  $A^*$ , while in the standard case these functions drop to zero, for the case of SDs we find that they have a minimum (very dependent upon the exact value of  $Q_{\text{SQM}}$ ) and tend to grow for lower values. This fact clearly shows that the pulsational properties of SDs and WDs should be deeply different.

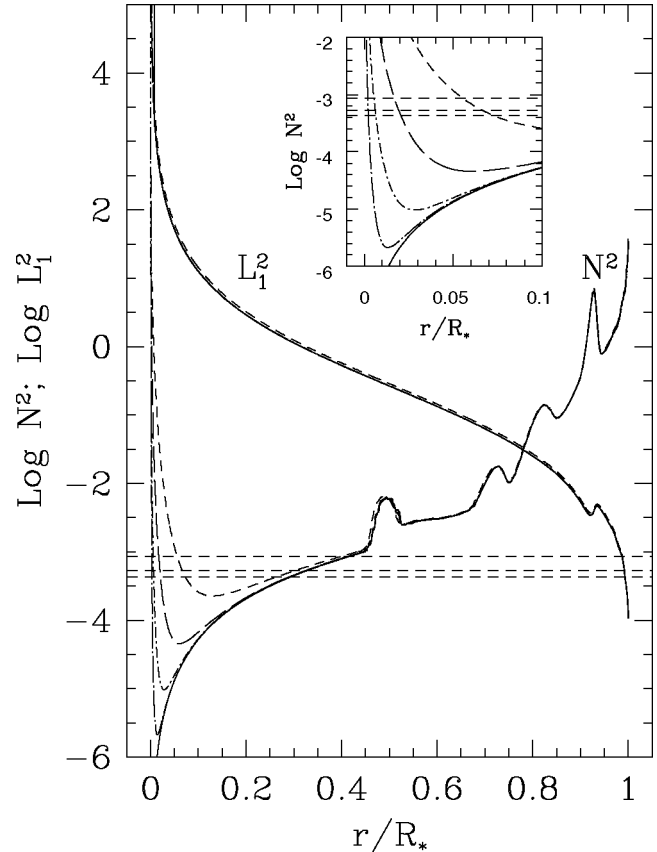


**Figure 5.** The ‘propagation diagram’ for models of SDs with  $Q_{\text{SQM}} = 10^{-2}$ ,  $10^{-3}$ ,  $10^{-4}$  and  $10^{-5}$  and for a standard WD model of the same mass. The lines have the same meaning as in Fig. 2. Curves labelled with  $N^2$  depict the Brunt–Väisälä frequency while the lines labelled with  $L_1^2$  represent the Lamb frequency for dipolar modes. The three horizontal dashed lines depict, in the scale of the figure, the three main modes (215, 271 and 307 s) observed in G117B15A. The regions for oscillatory behaviour are those in which  $\sigma^2 < N^2$ ;  $L_1^2$  (g-modes) or  $\sigma^2 > N^2$ ;  $L_1^2$  (p-modes). If these conditions are not fulfilled simultaneously, then we have an evanescent behaviour. Note that the presence of a SQM core gives rise to a sharp increase of the Brunt–Väisälä frequency very near the centre of the star. This, in turn, gives rise to the appearance of a further oscillatory cavity at the bottom of the normal matter part of the star. This supplementary cavity is responsible for the drastic changes (to be shown below) in the spectrum of non-radial oscillations of SDs as compared to standard WDs. In the inset, we show, in more detail, the Brunt–Väisälä frequency at the bottom of the normal matter portion of the considered models.

This is even more clear in Fig. 5 where we show the propagation diagram for the considered models. In the reference frame of the so-called local analysis [see section 15.2 of Unno et al. (1989)], we consider the coefficients of the equations of oscillation as constants and look for an exponential solution of the form  $\exp(ik_r r)$ , where  $k_r$  is given by

$$k_r^2 = \frac{(\sigma^2 - L_1^2)(\sigma^2 - N^2)}{c^2 \sigma^2}. \quad (17)$$

For an oscillating solution, we need  $k_r$  to be real. This will be fulfilled in two separate situations:  $\sigma^2 < N^2$ ;  $L_1^2$  (g-modes) or  $\sigma^2 > N^2$ ;  $L_1^2$  (p-modes). In zones in which none of these conditions is satisfied, the wave is exponentially decreasing. For the case of standard WDs, g-modes are oscillating in the outer part of the star. For example, for the case of the three modes observed in G117B15A,

these modes oscillate for  $r/R^* \gtrsim 0.40$  (see Fig. 5) while for layers with lower radii the waves are exponentially decreasing.

Now, the enormous modification of the innermost structure of the object due to the presence of a compact SQM core produces an extremely sharp increase in the Brunt–Väisälä frequency. As it is clear in Fig. 5, there appears a completely new region, near the SQM core, in which we simultaneously have  $\sigma^2 < N^2$ ;  $L_1^2$ , and, thus, this is a new region in which there is a true oscillatory behaviour. As a matter of fact, it is immediate to realize from equation (17) that the wave number of the waves in this region will be extremely short. Thus, *for period values in the range observed for DAVs the modes will have a very large number of nodes, and the order of the oscillation will be very large.* This is in sharp contrast with the well-known phenomenology of g-modes in standard WDs.

The calculations presented in this paper have been performed with a computed code tailored for computing pulsations of WDs. Consequently, we are employing the code in conditions very different from those attained in WD interiors, for which it is well tested. We feel it is fundamental to have at hand a simple model that reproduces the peak in the Brunt–Väisälä frequency near the SQM core. Such a model, based on very simplified physics, is presented in Appendix A. There, it is shown that the above-mentioned peak in the Brunt–Väisälä frequency is a real effect and not a numerical artifact. This result supports the numerical results presented in the main part of the paper.

Due to the very short wave number of the modes in the layers just outside the SQM core, it is adequate to treat the non-radial oscillations in the frame of an asymptotic analysis for modes with low  $\ell$  and high order. An important result of the asymptotic theory is that the separation of consecutive g-modes is given by

$$\sigma_n = \frac{\sqrt{\ell(\ell+1)}}{n\pi} \int_{r_a}^{r_b} \frac{N}{r} dr, \quad (18)$$

where  $r_a$  and  $r_b$  are the turning points at which we have  $k_r = 0$ . Now, for fixed limits of integration (as it is the case of sufficiently high order modes) we find that the separation of consecutive periods is constant.

In the case of SDs, the lower limit of the oscillating cavity will correspond to the lower limit of the fluid phase (see above). Now the spike in the integrand  $N/r$  is so sharp that consecutive modes will be *far closer* than for the case of standard WDs. This is a very distinctive characteristic of the pulsation of SDs that is directly comparable with observations.

#### 4 ASYMPTOTIC TREATMENT NEAR THE COMPACT CORE

From the results of the previous section, it is clear that the modes will have a strongly oscillating behaviour in the innermost cavity. Because of this reason, an asymptotic treatment of the problem for this region is very adequate. We believe so because in this case we will be able to separate two largely different behaviours, one in which the modes have a long wavelength (as it is usual for WDs in the standard cavity for g-modes) and another with extremely short wavelengths (in the innermost cavity due to the existence of the compact SQM core).

Specifically, we will try to get a function that will describe the modes throughout the entire innermost resonant cavity up to the evanescent zone which separates the inner and the standard resonant g-mode cavities. In doing so, we will employ this function as a boundary condition for performing a detailed, self-consistent numerical calculation of the eigenmodes for the entire stellar model.

In performing the asymptotic analysis of the modes, we will closely follow the treatment presented in Unno et al. (1989), and assume the Cowling approximation (i.e. we neglect the perturbations on the gravitational potential). We should remark that in the case of the very particular stellar models we are studying, and for the innermost resonant g-modes cavity, the Cowling approximation is almost exact. At these conditions, the solution of the equations of motion can be written in terms of the Airy functions as

$$y_{1,2} \propto (\alpha Ai(\zeta) + \beta Bi(\zeta)). \quad (19)$$

These functions can be approximated by means of their asymptotic expansions

$$\begin{aligned} \alpha Ai(\zeta) + \beta Bi(\zeta) &\approx \frac{1}{\sqrt{\pi(-\zeta)^{1/4}}} \left[ \frac{\alpha}{2} \exp\left(-\frac{2}{3}(-\zeta)^{3/2}\right) \right. \\ &\quad \left. + \beta \exp\left(\frac{2}{3}(-\zeta)^{3/2}\right) \right]; \quad (\zeta > 0) \\ \frac{1}{\sqrt{\pi\zeta^{1/4}}} &\left[ \alpha \cos\left(\frac{2}{3}\zeta^{3/2} - \frac{\pi}{4}\right) + \beta \sin\left(\frac{2}{3}\zeta^{3/2} - \frac{\pi}{4}\right) \right]; \quad (\zeta < 0). \end{aligned} \quad (20)$$

Here,  $\zeta$  is given by

$$\zeta = \text{sign}(k_r^2) \left[ \frac{3}{2} \int_{r_{\text{tp}}}^r |k_r| dr \right]^{2/3}, \quad (21)$$

where  $r_{\text{tp}}$  is the position of the turning point.

In the oscillating zone (below the turning point), we have  $\sigma \ll L_\ell$ ;  $N$ ; thus  $k_r \sim \sqrt{\ell(\ell+1)N}/\sigma r$ . On the contrary, in the evanescent zone we have  $L_\ell \gg \sigma$  and  $N \ll \sigma$ ; consequently  $k_r \sim \sqrt{\ell(\ell+1)}/r$ .

As stated before, at the bottom of the fluid phase we have to set the radial displacement to zero. This provides the equation

$$\beta = \alpha \tan \left[ \int_{r_{\text{tp}}}^{r_b} k_r dr - \frac{\pi}{4} \right], \quad (22)$$

where  $b$  stand for the bottom of the fluid phase.

Finally, the boundary conditions at the fitting point are given by

$$y_1 = \alpha \left[ \Theta + \frac{2}{\Theta} \tan \left( \frac{\sqrt{2}}{\sigma} \Gamma - \frac{\pi}{4} \right) \right], \quad (23)$$

$$y_2 = \alpha \frac{\sigma^2 r_f}{g} \left[ \Theta \tan \left( \frac{\sqrt{2}}{\sigma} \Gamma - \frac{\pi}{4} \right) - \frac{1}{\Theta} \right]. \quad (24)$$

Here,  $\Theta$  is given by

$$\Theta = \left( \frac{r_f}{r_{\text{tp}}} \right)^{\sqrt{2}} \quad (25)$$

and

$$\Gamma = \int_{r_{\text{tp}}}^{r_f} \frac{N}{r} dr. \quad (26)$$

The value of the amplitude  $\alpha$  will be found as one of the results of the numerical calculation of the g-modes for the whole stellar model.

#### 5 NUMERICAL RESULTS

In this section, we will describe the results found in computing the dipolar g-modes for the full stellar models. Here, we employ the boundary conditions given by equations (23) and (24) for the bottom of the grid in which we divided the stellar model.

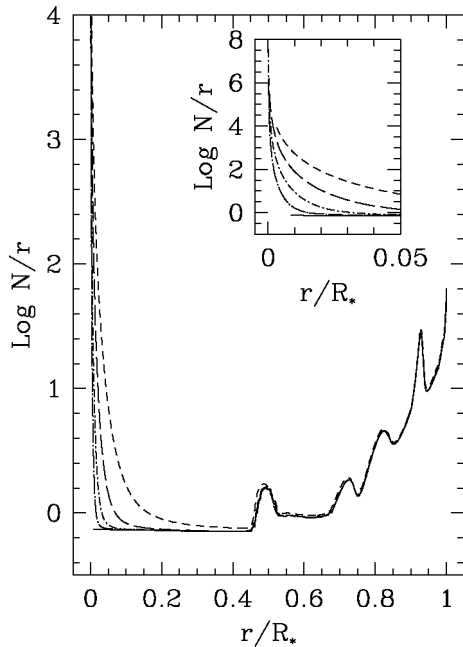


**Figure 6.** The Brunt–Väisälä frequency over the radius of the star for models of SDs with  $Q_{\text{SQM}} = 10^{-2}, 10^{-3}, 10^{-4}$  and  $10^{-5}$  and for a standard WD of the same mass. Lines have the same meaning as in Fig. 2. In the inset, we show in more detail the profile of this function at the bottom of the normal matter portion of the models considered here. The integral of this function between turning points provides the period separation between consecutive modes.

The numerical calculation of the spectrum is very time consuming because of the enormous number of g-modes found in the period interval detected in variable WDs. Because of this reason, we will restrict ourselves to modes with periods between 150 and 500 s. The main numerical results we found are presented in Figs 7–10 where we display the period spacing of consecutive modes, the coefficient  $\alpha$  of equations (23) and (24) and the amplitude of the eigenfunction  $y_2$  at the stellar surface as a function of the period of the modes.

In all the considered cases ( $Q_{\text{SQM}} = 10^{-2}, 10^{-3}, 10^{-4}$ , and  $10^{-5}$ ), we find that the period spacing between consecutive modes is below 1 s. This is in sharp contrast with the case of the same stellar model without any SQM core (shown in Fig. 11), for which period spacing is few tens of seconds. For all the period interval considered, we find  $y_2$  at the stellar surface (proportional to horizontal displacement) is of the order of the radial displacement. Remarkably, the shortest period spacing corresponds to the case of  $Q_{\text{SQM}} = 10^{-4}$ . This is due to the fact that for such a SQM core mass fraction, there occurs the sharpest peak in the Brunt–Väisälä in non-crystallized normal matter.

The coefficient  $\alpha$  which is proportional to the amplitude of the oscillation at the inner resonant cavity is a function that undergoes a sharp variation in the considered period interval. The square of this amplitude is directly related to the energy associated with the modes. Thus, modes with periods near to any of the minima should be far easier to excite than others between consecutive minima. Thus, the spectrum of dipolar oscillations of SDs should be characterized by several clusters of modes well separated by each other. These minima correspond to period values at which the outer, normal matter envelope has a node at the fitting point. This is largely determined by the structure of these normal layers. Each of these clusters should be formed by a large number of modes nearly evenly spaced.

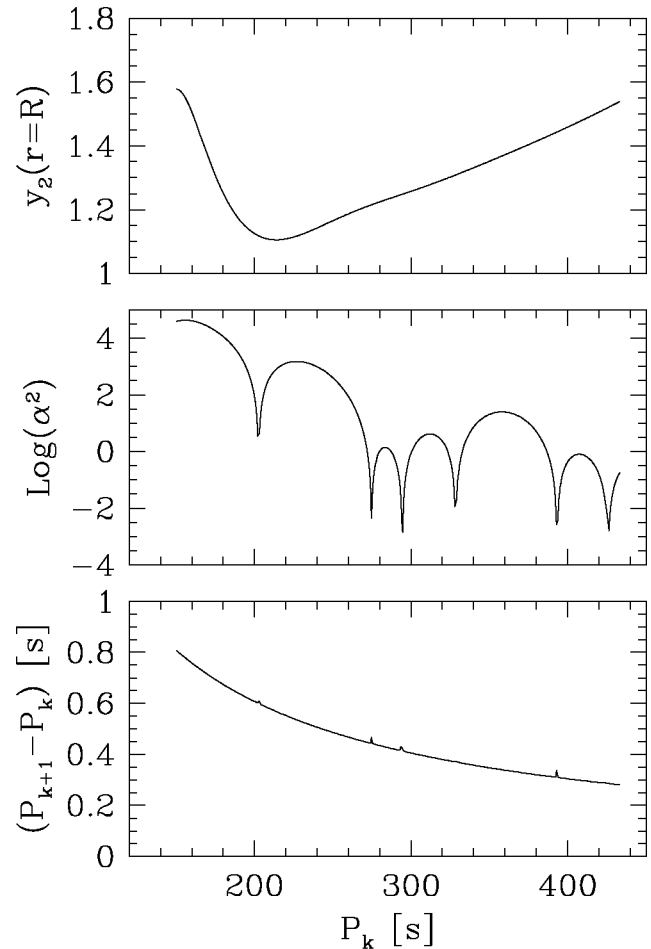


**Figure 7.** Period spacing of consecutive modes (bottom panel), the coefficient  $\alpha$  of equations (23) and (24) (middle panel) and the amplitude of the eigenfunction  $y_2$  at the stellar surface (upper panel) as a function of the period of the modes for the case of  $Q_{\text{SQM}} = 10^{-2}$ .

## 6 DISCUSSION AND CONCLUSIONS

From the results presented above, it is clear that the spectrum of non-radial pulsations of strange dwarf stars (SDs) is completely different from the one expected for a standard WDS without any compact core. We find that the spectrum of dipolar oscillations of SDs should be characterized by several clusters of modes well separated by each other. These clusters should be located on the minimum of the amplitudes at the fitting point we considered (at  $\approx 0.10 R$ , see previous sections for further details) which are shown in the middle panels of Figs 7–10. At these period values, we have a small amplitude for the oscillations near the SQM core, which will allow them to reveal at the stellar surface with a noticeable amplitude. Also, at these periods, the kinetic energy associated to the modes will be far lower than for other modes with larger amplitudes (note the logarithmic vertical scale of the middle panels of Figs 7–10).

Inside the cluster of modes, we expect the occurrence of a large number of modes nearly evenly spaced. This is the very characteristic of SDs. In the case of a rotating WD, we should expect a splitted triplet (related to the azimuthal quantum number  $m = -1, 0, 1$ ). Here, the number of modes inside each cluster should be so large that they cannot be interpreted as due to, e.g., rotation (we would need to have a very large harmonic degree  $\ell$ ). Consequently, this should be considered as a direct evidence of the presence of a

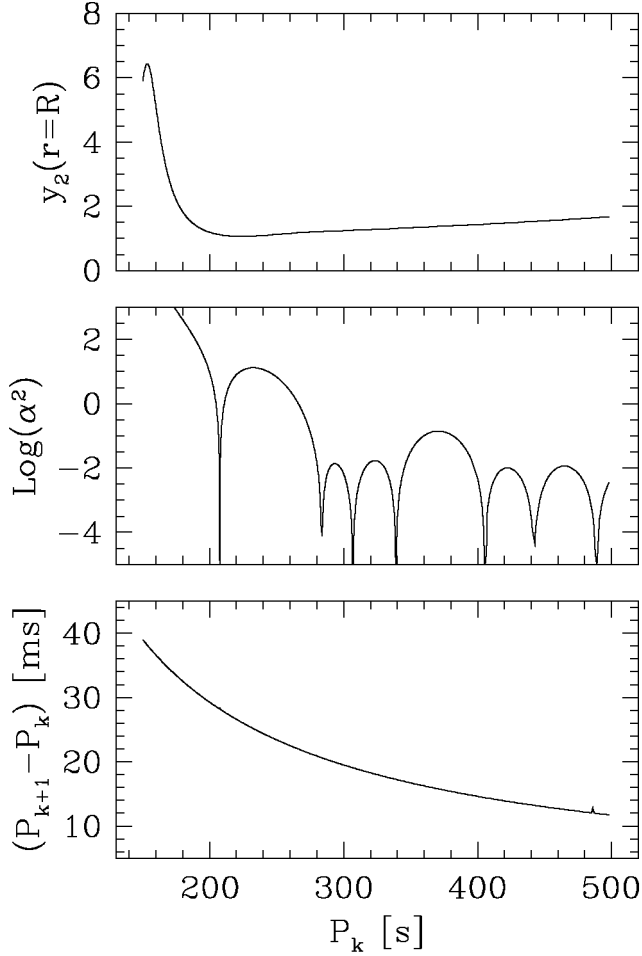


**Figure 8.** Same as Fig. 7 but for the case of  $Q_{\text{SQM}} = 10^{-3}$ .

high-density SQM inside a WD. Thus, these results may be considered as a direct indication that, in some sense, WDs may be envisaged as SQM detectors as recently proposed in Paper I.

A relevant point is related to the conditions at which observations of variable WD would be able to reveal the existence of a SQM compact core. As discussed above, we have found that there should exist cluster of modes separated by large gaps in period. However, in order to estimate the actual number of modes excited to observable amplitudes in each cluster we have to perform a deeper analysis considering the energetics of the modes in SDs. We plan to present such study in a subsequent publication. In any case, we can perform a preliminary estimation of the requirements for an observation to be useful in detecting a SQM core. We arbitrarily considered a signal containing a cluster of 20 modes of equal amplitude and evenly spaced in frequency with spacing  $\Delta\omega = 0.01$ , centred in  $\omega = \omega_0$  and performed its Fourier transform to get the spectrum of frequencies  $A(\omega)$ . If  $T$  represents the time interval of observations, we find that the structure of modes of the cluster is noticeable for  $T \approx 900$  (see Fig. 12). In other words, we need  $\Delta\omega T \approx 10$ . We can employ this result in order to estimate the minimum length of observation to reveal the presence of a SQM core, we find  $T \gtrsim 110(P/100 \text{ s})^2(\Delta P/1 \text{ ms})^{-1} \text{ d}$ , where  $\Delta P$  corresponds to  $P_{k+1} - P_k$ . For a cluster of modes centred at  $P = 300 \text{ s}$ , we find that (employing the  $\Delta P$  values given in the previous section)  $T$  should be larger than 2, 50, 200 and 10 d for the cases of  $Q_{\text{SQM}} =$

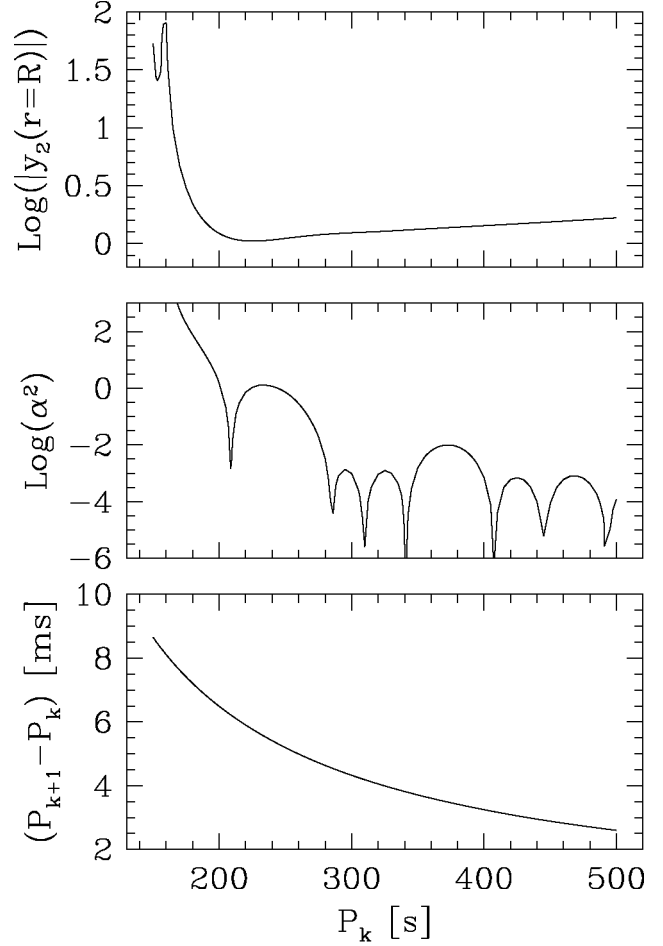


**Figure 9.** Same as Fig. 7 but for the case of  $Q_{\text{SQM}} = 10^{-4}$ .

$10^{-2}$ ,  $10^{-3}$ ,  $10^{-4}$  and  $10^{-5}$ , respectively. We think that by employing the Whole Earth Telescope (see e.g. Winget et al. 1990) it is possible to perform an analysis with the hope of detecting a period clustering like the one found here even with the presently available observational facilities. In any case, note that, in performing this rough estimation we have considered ideal data without any noise; clearly we need a further study of the detectability of SQM cores in WDs.

Finally, we should remark that intermediate mass WDs ( $M_{\text{WD}} \approx 0.6 M_{\odot}$ ) are particularly suitable as SQM detectors because the compression in the bottom of the normal matter envelope is not strong enough to induce full crystallization [see fig. 12 of Benvenuto & Althaus (1996a)]. However, in massive WDs ( $M_{\text{WD}} \approx 1.0 M_{\odot}$ ) the effects due to the presence of a SQM core on the oscillation spectrum will be barely noticeable. In such a case, for the range of effective temperatures at which variable WDs are observed, theory predicts that even standard WDs should have already crystallized a large portion of the star. If a SQM core is present, the crystallized portion of the star will be even larger. This inhibits the oscillation of the layers in which the Brunt–Väisälä frequency peak occurs, and thus the effect on the oscillation spectrum induced by a SQM will be hardly distinguishable.

#### ACKNOWLEDGMENTS

The author warmly acknowledges Prof. Héctor Vucetich for enlightening discussions on the topic of this work. He also thanks the referee, Prof. Phillip Podsiadlowski, for his report that has been very



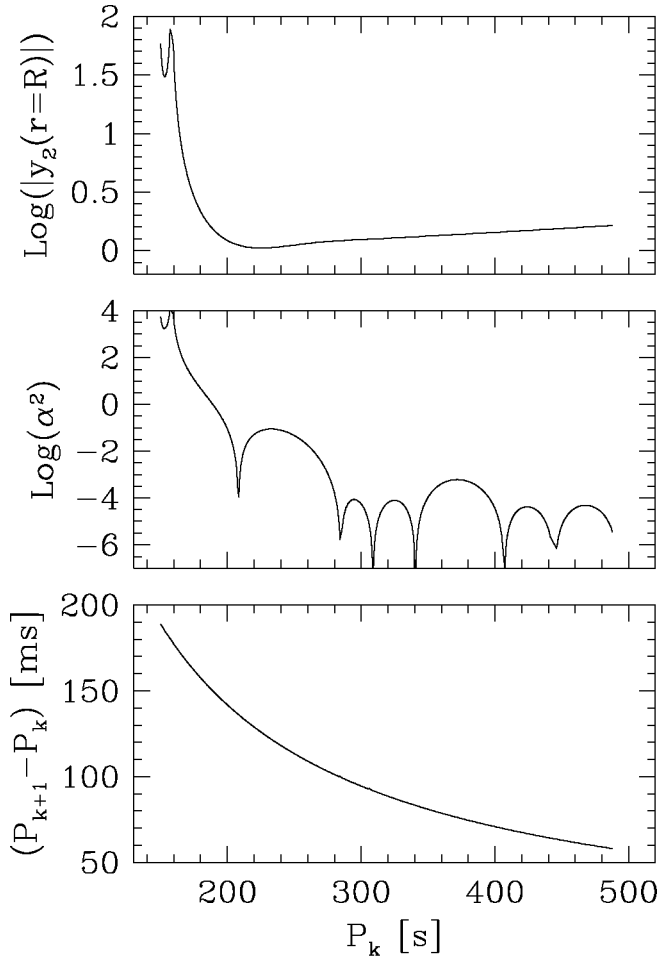


Figure 10. Same as Fig. 7 but for the case of  $Q_{SQM} = 10^{-5}$ .

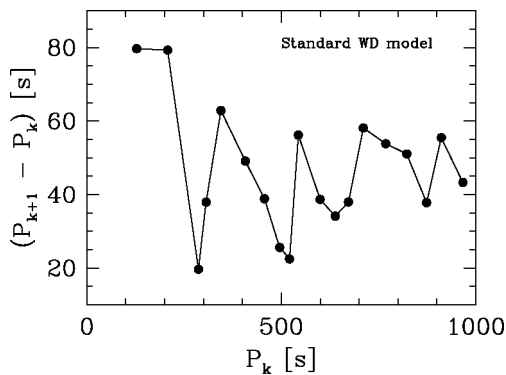


Figure 11. The period separation of consecutive dipolar modes for a standard carbon–oxygen WD star of 0.525 as a function of the pulsation period. Solid dots denote the position of the modes.

useful in improving the original version of the present work. OGB has been supported by FONDAF Center for Astrophysics 1501003.

## REFERENCES

- Alcock C., Olinto A., 1990, *Annu. Rev. Nucl. Part. Sci.*, 38, 161  
 Benvenuto O. G., 2005, *J. Phys. G*, 31, L13 (Paper I)  
 Benvenuto O. G., Althaus L. G., 1996a, *ApJ*, 462, 364  
 Benvenuto O. G., Althaus L. G., 1996b, *Phys. Rev. D*, 53, 635

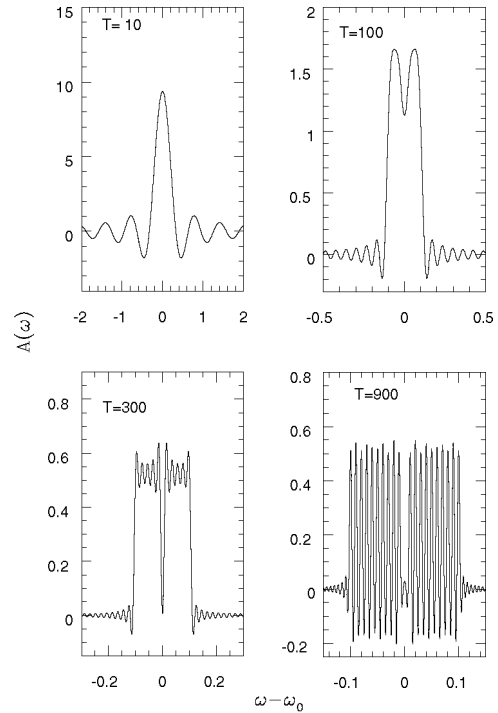


Figure 12. The Fourier transform  $A(\omega)$  of a cluster of 20 modes of equal amplitude and evenly spaced in frequency with spacing  $\Delta\omega = 0.01$ , centred in  $\omega = \omega_0$ .  $T$  represents the time interval of observations. Note that in order to find the structure of a cluster of frequencies we need to have data for  $T \approx 900$ . For further details, see the text.

- Benvenuto O. G., Horvath J. E., 1989, *Phys. Rev. Lett.*, 63, 716  
 Benvenuto O. G., Córscico A. H., Althaus L. G., Serenelli A. M., 2002, *MNRAS*, 332, 399  
 Benvenuto O. G., García-Berro E., Isem J., 2004, *Phys. Rev. D*, 69, 082002  
 Bodmer A. R., 1971, *Phys. Rev. D*, 4, 1601  
 Bradley P. A., 1998, *ApJS*, 116, 307  
 Buras R., Rampp M., Janka H.-T., Kifonidis K., 2003, *Phys. Rev. Lett.*, 90, 241101  
 Córscico A. H., Benvenuto O. G., Althaus L. G., Isem J., García-Berro, E., 2001, *New Astron.*, 6, 197  
 Drake J. J. et al., 2002, *ApJ*, 572, 996  
 Farhi E., Jaffe R. L., 1984, *Phys. Rev. D*, 30, 2379  
 Glendenning N. K., Kettner C., Weber F., 1995a, *Phys. Rev. Lett.*, 74, 3519  
 Glendenning N. K., Kettner C., Weber F., 1995b, *ApJ*, 450, 253  
 Han Z., Podsiadlowski P., Eggleton P. P., 1994, *MNRAS*, 270, 121  
 Horvath J. E., Benvenuto O. G., 1988, *Phys. Lett. B*, 213, 516  
 Isem J., Hernanz M., Garcia-Berro E., 1992, *ApJ*, 392, L23  
 Kepler S. O., Mukadam A., Winget D. E., Nather R. E., Metcalfe T. S., Reed M. D., Kawaler S. D., Bradley P. A., 2000, *ApJ*, 534, L185  
 Lang K. N., 1999, *Astrophysical Formulae*, Vol. I. Springer, Berlin  
 Li X.-D., Bombaci I., Dey M., Dey J., van den Heuvel E. P. J., 1999, *Phys. Rev. Lett.*, 83, 3776  
 Metcalfe T. S., Montgomery M. H., Kanaan A., 2004, *ApJ*, 605, L133  
 Page D., Uslov V. V., 2002, *Phys. Rev. Lett.*, 89, 131101  
 Panei J. A., Althaus L. G., Benvenuto O. G., 2000, *A&A*, 353, 970  
 Terazawa H., 1979, *INS-Report-338* (INS, Univ. of Tokyo)  
 Unno W., Osaki Y., Ando H., Saio H., Shibahashi H., 1989, *Nonradial Oscillations of Stars*, 2nd ed. Univ. of Tokyo Press, Tokyo  
 Vartanyan Y. L., Grigoryan A. K., Sargsyan T. R., 2004, *Astrophysics*, 47, 189  
 Winget D. E. et al., 1990, *ApJ*, 357, 630  
 Witten E., 1984, *Phys. Rev. D*, 30, 272  
 Xu R. X., 2002, *ApJ*, 570, L65

### APPENDIX A: AN APPROXIMATE, ANALYTIC TREATMENT OF THE BRUNT-VÄISÄLÄ FREQUENCY NEAR THE SUPERDENSE CORE

In the case of SDs, the object attains conditions of higher densities and steeper slopes in most of the relevant physical quantities compared to the case of a standard WD object. Then, in our opinion, it is highly desirable to have at hand an analytic, approximate treatment for the Brunt–Väisälä frequency at the bottom of the normal matter envelope to be confident with the numerical results provided by a code working at conditions at which it has not been tested previously. We should remark that there the Brunt–Väisälä frequency shows a steep increase, which is responsible for g-mode resonance at these layers.

In order to keep the analytic treatment as simple as possible, here we will consider the plasma as a mixture of ideal nuclei together with degenerate electrons, neglecting the Coulomb corrections, but keeping thermal effects to second order.<sup>3</sup> Moreover, as at these layers the density is high enough to consider that the electron gas is relativistic.

We found it convenient to employ an expression for the Brunt–Väisälä frequency different from equation (13) (Lang 1999, p. 320)

$$N^2 = \frac{g \delta}{C_p} \frac{dS}{dr}, \quad (\text{A1})$$

where  $C_p$  is the specific heat at constant pressure and  $S$  is the specific entropy, both per gram of stellar material, and

$$\delta = - \left. \frac{\partial \ln \rho}{\partial \ln T} \right|_P. \quad (\text{A2})$$

As it is well known, at the very high degree of degeneracy present at these stellar layers, pressure is dominated by electron degeneracy, while thermal effects are due to non-degenerate nuclei. Then, neglecting the contributions of degenerate electrons we have

$$C_p = \frac{3}{2} \frac{R}{\mu_0}, \quad (\text{A3})$$

where  $\mu_0$  is the mean molecular weight per nuclei defined as  $1/\mu_0 = \sum_i X_i/A_i$  ( $X_i$  and  $A_i$  are the mass fraction and the atomic weight of the  $i$  component of the plasma) and the entropy is

$$S = \frac{R}{\mu_0} \ln \left( \frac{\rho}{\mu_0 m_p} \right) + \frac{3}{2} \frac{R}{\mu_0} \ln(kT) + \frac{R}{\mu_0} \left\{ \frac{5}{2} + \ln \left[ g_0 \left( \frac{2\pi m_p}{h^2} \right)^{3/2} \right] \right\}, \quad (\text{A4})$$

where symbols have their standard meaning. Taking the derivative of the entropy, we find

$$\frac{dS}{dr} = \frac{3}{4} \frac{R}{\mu_0} \frac{g\rho}{P} (1 - 2\nabla), \quad (\text{A5})$$

where  $\nabla = \partial \ln T / \partial \ln P$ .

In computing  $\delta$  we will consider that the pressure and density are given by

$$P = \frac{R}{\mu_0} \rho T + \frac{m^4 c^5}{6\pi^2 \hbar^3} \left[ \frac{x^4}{2} + \pi^2 \left( \frac{kT}{mc^2} \right)^2 x^2 \right] \quad (\text{A6})$$

<sup>3</sup> This is essential, since at  $T = 0$ , the Brunt–Väisälä frequency vanishes.

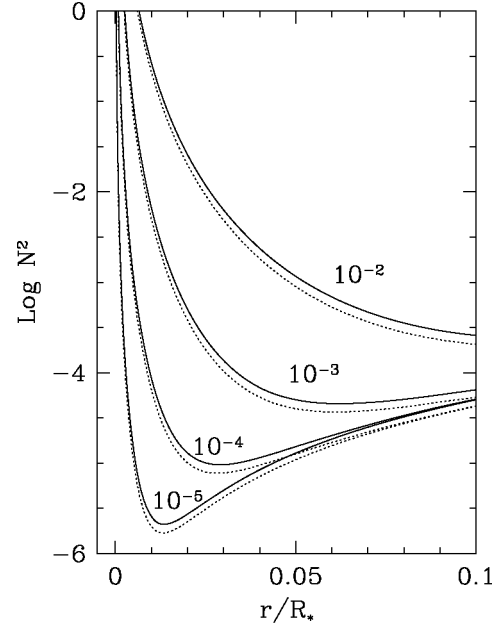


**Figure A1.** A comparison of the numerical calculation of the Brunt–Väisälä frequency at the bottom of the normal matter envelope (solid lines) with the analytic treatment given by equations (A1), (A3), (A5) and (A8) (dotted lines). Curves are labelled with their corresponding value of  $Q_{\text{SQM}}$

and

$$\rho = \frac{2m_p}{3\pi^2} \left( \frac{mc}{\hbar} \right)^3 \left[ x^3 + \pi^2 \left( \frac{kT}{mc^2} \right)^2 x \right], \quad (\text{A7})$$

where we assumed a molecular weight per electron  $\mu_e = 2$ . Calculating the derivative up to second order in temperature, we find

$$\delta = \frac{6m_p}{mc^2} \frac{R}{\mu_0} \frac{T}{x} + \frac{3\pi^2}{x^2} \left( \frac{kT}{mc^2} \right)^2. \quad (\text{A8})$$

Now, we are in a position to compute the Brunt–Väisälä frequency provided by the analytic treatment. Considering the SD models described in the main part of the text, we calculate  $N^2$  by employing equations (A1), (A3), (A5) and (A8) and considering these layers as isothermal ( $\nabla = 0$ ). The results are displayed in Fig. A1 where it can be noted that the analytic calculations are very close to the numerical results for a wide range of values of masses of the SQM compact core. The differences between both treatments should be attributed to the fact that in the analytic we have ignored interactions and the temperature gradient. In fact,  $\nabla T \neq 0$  because of the neutrino emissivity of the SQM core.

From these results, it is clear that the peak in the Brunt–Väisälä frequency at the bottom of the normal matter envelope is a real effect and not a numerical artifact. This justifies the treatment performed in the main part of the present paper.

This paper has been typeset from a T<sub>E</sub>X/L<sup>A</sup>T<sub>E</sub>X file prepared by the author.